On the concept of macroscopic capillary pressure in two-phase porous media flow

Authors

M. Starnoni[1,2], D. Pokrajac[1]

[1] School of Engineering, University of Aberdeen, Aberdeen, Scotland, United Kingdom

[2] Department of Mathematics, University of Bergen, Bergen, Norway

Corresponding author: michele.starnoni@uib.no

Abstract

Although two-phase fluid flow in porous media has been an established research field for decades, its theoretical background is still incomplete. In particular, while a universal definition of capillary pressure exists at the micro-scale, its upscaling to the macro-scale is still rather vague. In this work, a clear and rigorous definition of the macroscopic capillary pressure is proposed, which follows naturally from application of the method of volume averaging to interface properties in multiphase systems. The relationship between the macroscopic capillary pressure and the average properties of the medium is given by the macroscopic momentum balance for the fluid-fluid interfaces, in a form which can be interpreted as a generalized Young-Laplace equation at the macro-scale. We then present simulation results of drainage in a porous region extracted from a three-dimensional micro-CT image of a real carbonate rock, and show how our formulation differs from the standard one which is commonly employed in field-scale computational codes.

Key points

- A new definition of the macroscopic capillary pressure is presented
- The definition follows from rigorously averaged microscopic pressures in two fluid phases
- Simulation results of drainage on a micro-CT image of a carbonate rock are shown

1 Introduction

In classic theory of two-phase flow of immiscible fluids in porous media, capillary pressure p_c is defined as (Scheidegger, 1963; Bear, 1972)

$$p_c = p_n - p_w, \tag{1}$$

where p_n and p_w are the pressures of the non-wetting and wetting phases on their respective side of the interface. The relationship between capillary pressure, surface tension σ and mean interface curvature k is given by the Young-Laplace equation:

$$p_c = \sigma k, \tag{2}$$

However, while definition (1) is universal, its upscaling to the macro-scale is still rather vague, and a rigorous theory of capillarity at the macro-scale is lacking. The standard approach is to define the macroscopic capillary pressure $\mathcal{P}_c$ in analogy with its microscopic definition as (Whitaker, 1977; Bear and Verruijt, 1987)

$$\mathcal{P}_c = \langle p_n \rangle^n - \langle p_w \rangle^w, \tag{3}$$

where $\langle p_\alpha \rangle^\alpha$, $\alpha = n, w$, is the intrinsic volume average of the pressure. $\mathcal{P}_c$ is then expressed using functional relationships of the kind

$$\mathcal{P}_c = \mathcal{F}(s_w), \tag{4}$$

where s_w is the saturation of the wetting phase. The $\mathcal{P}_c - s_w$ relationhip is usually obtained through laboratory experiments, e.g. the Brooks-Corey curve (Brooks and Corey, 1964) or Van Genuchten's model (Van Genuchten, 1980), and is employed in all modern continuum-based numerical codes for subsurface multiphase flow simulations, e.g. TOUGHREACT (Xu et al., 2011), HYTEC (Van Der Lee et al., 2003), HYDROGEOCHEM (Yeh and Tripathi, 1990). The fact that such a functional relationship is now widely established even if lacking theoretical basis, is mainly due to two practical reasons. Firstly, it provides a simple relationship between pressure within the phases in macro-scale models for porous media flows. Secondly, capillary pressure in this form can be efficiently calculated from

coreflooding experiments simply as the difference between the pressures at both ends of the core. As a result constitutive $P_c - s_w$ relationships can be easily obtained and incorporated into the computational models.

Other authors (Morrow, 1970; Allen, 1986; Hassanizadeh and Gray, 1993) have seeked a thermodynamic basis of capillary pressure at the macro-scale. On one hand, thermodynamic definitions of the macroscopic capillary pressure are undoubtably more theoretically sound than simple empirical functions of saturation, but on the other hand, they result from constitutive hypotheses which are axiomatically introduced at the macro-scale.

In this paper we use rigorous theory of volume averaging to provide a new formulation of the macroscopic capillary pressure in porous media flows. The paper is organized as follows. First, basic notation is introduced in Sec. 2 to facilitate presentation of equations in the remainder of the paper. The microscopic momentum balance for the fluid-fluid interfaces, namely the generalized Young-Laplace equation, is presented in Sec. 3. In Sec. 4 a review of the approaches commonly employed to define capillary pressure at the macro-scale is given. The proposed theory is presented in Sec. 5. In Sec. 6 simulation results of pore-scale two-phase flow in a porous region extracted from a real reservoir rock are presented, and a comparison of different definitions of macroscopic capillary pressure is made. After a discussion on the limitations of the proposed approach in Sec. 7, concluding remarks are given in Sec. 8.

2 Definitions and notation

Considering the surface $\mathcal{S}$ having boundary $\mathcal{C}$ depicted in Fig. 1, a set of orthogonal unit vectors $\boldsymbol{\ell}$, $\mathbf{m}$ and $\mathbf{n}$, where $\mathbf{n}$ is the unit normal to the surface, is defined. At the boundary $\mathcal{C}$, $\boldsymbol{\ell}$ is tangent to $\mathcal{C}$, and $\mathbf{m}$ is both tangent to $\mathcal{S}$ and normal to $\mathcal{C}$ pointing outwards from $\mathcal{C}$, so that at the boundary $\mathbf{m} \cdot \mathbf{n} = 0$. The surficial components Ψ_s^s of the general vector quantity Ψ_s defined on the surface, is given by

$$\Psi_{\mathbf{s}}^{\mathbf{s}} = \Psi_{\mathbf{s}} - \mathbf{nn} \cdot \Psi_s, \tag{5}$$

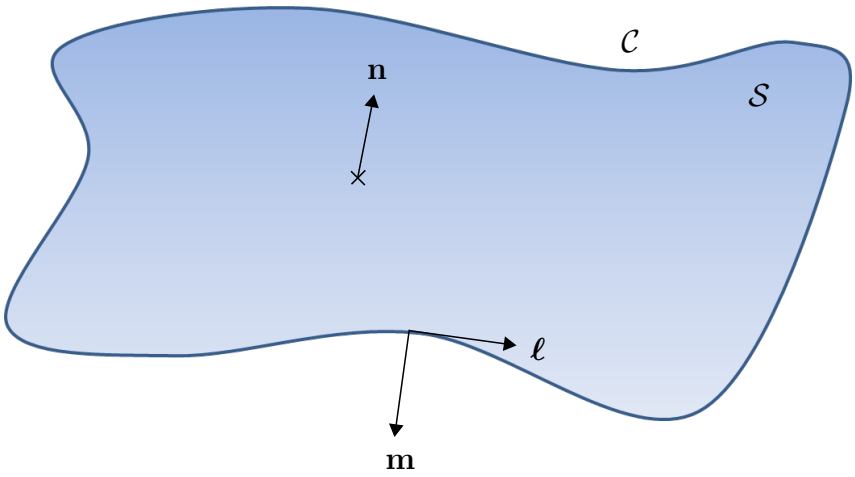

Figure 1. General surface $\mathcal{S}$ with boundary $\mathcal{C}$ and the set of orthogonal unit vectors $\boldsymbol{\ell}$, $\mathbf{m}$ and $\mathbf{n}$, where $\mathbf{n}$ is the unit normal to the surface and $\boldsymbol{\ell}$ and $\mathbf{m}$ are constrained to be orthogonal to $\mathbf{n}$ and to each other. At the boundary $\mathcal{C}$, $\boldsymbol{\ell}$ is tangent to $\mathcal{C}$ and $\mathbf{m}$ is both tangent to $\mathcal{S}$ and normal to $\mathcal{C}$ pointing outwards from $\mathcal{S}$

where the product $\mathbf{nn}$ is the dyadic product. In the same way, the surficial components $\mathbf{I}^s$ and ∇^s of the identity tensor $\mathbf{I}$ and operator ∇ respectively, are given by

$$\mathbf{I}^s = \mathbf{I} - \mathbf{nn} \cdot \mathbf{I}, \tag{6}$$

$$\nabla^s = \nabla - \mathbf{nn} \cdot \nabla. \tag{7}$$

Let $\mathcal{S}_{\alpha\beta}$ be a surface of discontinuity between two phases α and β, its area is given by

$$a_{\alpha\beta} = \int_{\mathcal{S}_{\alpha\beta}} dA. \tag{8}$$

The surface intrinsic average of the general microscopic quantity $\psi_{\alpha\beta}$ associated with the surface $\mathcal{S}_{\alpha\beta}$ is defined as (Whitaker, 1969)

$$\langle \psi_{\alpha\beta} \rangle^{\alpha\beta} = \frac{1}{a_{\alpha\beta}} \int_{\mathcal{S}_{\alpha\beta}} \psi_{\alpha\beta} dA. \tag{9}$$

The surface integral over $\mathcal{S}_{\alpha\beta}$ can be converted into a volume integral over a volume $\forall$ containing $\mathcal{S}_{\alpha\beta}$, by means of the Dirac's delta function $\delta_{\alpha\beta}$ in the following way

$$\int_{\mathcal{S}_{\alpha\beta}} \psi_{\alpha\beta} dA = \int_{\forall} \psi_{\alpha\beta} \delta_{\alpha\beta} dV, \tag{10}$$

where $\delta_{\alpha\beta}$ is defined for any position $\mathbf{x}$ within $\forall$, such as

$$\begin{aligned} \delta_{\alpha\beta}(\mathbf{x}) = 0, \quad \mathbf{x} \notin \mathcal{S}_{\alpha\beta} \\ \int_{\forall} \delta_{\alpha\beta}(\mathbf{x}) dV = 1. \end{aligned} \tag{11}$$

Using eq. (10), an additional averaging measure called here superificial surface average is introduced as

$$\langle \psi_{\alpha\beta} \rangle = \frac{1}{\forall} \int_{\forall} \psi_{\alpha\beta} \delta_{\alpha\beta} dV = \frac{1}{\forall} \int_{\mathcal{S}_{\alpha\beta}} \psi_{\alpha\beta} dA, \tag{12}$$

It is worth noting that the integration volume $\forall$ is assumed to be of size of at least the Representative Elementary Volume (REV) (Bear, 1972) for the material. Surface spatial decomposition is defined as

$$\psi_{\alpha\beta} = \langle \psi_{\alpha\beta} \rangle^{\alpha\beta} + \tilde{\psi}_{\alpha\beta}, \tag{13}$$

where the quantity $\tilde{\psi}_{\alpha\beta}$ is called the spatial deviation of $\psi_{\alpha\beta}$, (for well-behaved quantities $\langle \tilde{\psi}_{\alpha\beta} \rangle = 0$). Finally, the specific surface area $\hat{a}_{\alpha\beta}$ is given by

$$\hat{a}_{\alpha\beta} = \frac{a_{\alpha\beta}}{\forall}, \tag{14}$$

and the relationship between the intrinsic surface average and the superficial surface average is

$$\langle \psi \rangle_{\alpha\beta} = \hat{a}_{\alpha\beta} \langle \psi_{\alpha\beta} \rangle^{\alpha\beta}. \tag{15}$$

Discussion on the role of specific surface area as macroscopic state variable can be found in Joekar-Niasar and Hassanizadeh (2011).

2.1 Theorems

The following integration theorems are formulated for a general function ψ_s defined on a surface contained within an averaging volume $\forall$ (Gray and Hassanizadeh, 1989; Gray et al., 1993)

$$\langle\frac{\partial\psi_s}{\partial t}\rangle = \frac{\partial}{\partial t}\langle\psi_s\rangle + \nabla\cdot\langle\mathbf{n}v_n^s\psi_s\rangle + \langle kv_n^s\psi_s\rangle - \frac{1}{\forall}\int_{\mathcal{C}}\mathbf{m}\cdot\mathbf{w}\psi_s dC, \tag{16a}$$

$$\langle\nabla^s\psi_s\rangle = \nabla\langle\psi_s\rangle - \nabla\cdot\langle\mathbf{nn}\psi_s\rangle - \langle k\mathbf{n}\psi_s\rangle + \frac{1}{\forall}\int_{\mathcal{C}}\mathbf{m}\psi_s dC, \tag{16b}$$

$$\langle\nabla^s\cdot\Psi_s\rangle = \nabla\cdot\langle\Psi_s^s\rangle - \langle k\mathbf{n}\cdot\Psi_s\rangle + \frac{1}{\forall}\int_{\mathcal{C}}\mathbf{m}\cdot\Psi_s dC. \tag{16c}$$

where $\mathbf{w}$ is the velocity of $\mathcal{C}$ and $v_n^s =$ is the speed of displacement, i.e. the velocity in the direction of $\mathbf{n}$ of a fluid particle contained within the surface, defined as

$$\mathbf{u}_s\cdot\mathbf{n} = v_n^s, \tag{17}$$

where $\mathbf{u}_s$ is the particle surface velocity, i.e. the time rate of change of its spatial position.

3 Generalized Young-Laplace equation

For a body consisting of two bulk phases α and β separated by a surface with unit normal $\mathbf{n}$, the microscopic mass and momentum conservation equations read (Deemer and Slattery, 1978)

$$\frac{\partial\rho_s}{\partial t} + \nabla^s\cdot(\rho_s\mathbf{u}_s) + [\![\rho(\mathbf{u}-\mathbf{u}_s)\cdot\mathbf{n}]\!]_\alpha^\beta = 0, \tag{18}$$

$$\frac{\partial}{\partial t}(\rho_s\mathbf{u}_s) + \nabla^s\cdot(\rho_s\mathbf{u}_s\mathbf{u}_s) - \nabla^s\cdot\mathbf{t}_s - \rho_s\mathbf{g} + [\![\rho\mathbf{u}(\mathbf{u}-\mathbf{u}_s)\mathbf{n} - \mathbf{tn}]\!]_\alpha^\beta = 0, \tag{19}$$

where ρ_s is the surface density with units of mass per unit area, $\mathbf{u}$ is the velocity of the bulk phase, $\mathbf{u}_s$ is the surface velocity, $\mathbf{t}$ and $\mathbf{t}_s$ are the stress tensors for the bulk phase and surface respectively, $\mathbf{g}$ is the acceleration due to gravity, and the operator $[\![\mathbf{Bn}]\!]_\alpha^\beta$ is the jump condition across the interface

$$[\![\mathbf{Bn}]\!]_\alpha^\beta = \mathbf{B}_\alpha\mathbf{n}_{\alpha\beta} + \mathbf{B}_\beta\mathbf{n}_{\beta\alpha},$$

where $\mathbf{n}_{\alpha\beta}$ is unit normal vector pointing from the α phase into the β phaseC. For the sake of clarity, it is remarked that velocities and stress tensors of the bulk phases are represented in this double bracketed term. Applying the chain rule to the first two terms of eq. (19) and combining with the mass balance, the momentum equation is rearranged

as

$$\rho_s \frac{D_s \mathbf{u}_s}{Dt} - \nabla^s \cdot \mathbf{t}_s - \rho_s \mathbf{g} + [\![\rho(\mathbf{u}-\mathbf{u}_s)(\mathbf{u}-\mathbf{u}_s)\mathbf{n} - \mathbf{t}\mathbf{n}]\!]_\alpha^\beta = 0. \tag{20}$$

The stress tensors for the bulk phase $\mathbf{t}$ and for the interface $\mathbf{t}_s$ take the form

$$\mathbf{t} = -p\mathbf{I} + \boldsymbol{\tau} \qquad \text{with units F } L^{-2}, \tag{21a}$$

$$\mathbf{t}_s = \sigma \mathbf{I^s} + \boldsymbol{\tau}_s \qquad \text{with units F } L^{-1}, \tag{21b}$$

where p is the pressure, $\boldsymbol{\tau}$ and $\boldsymbol{\tau}_s$ are the viscous stress tensors for the bulk phase and the interface respectively, σ is the interfacial tension, $\mathbf{I}$ is the identity tensor, and $\mathbf{I}^s$ is the surficial identity tensor defined by eq. (6).

Substituting eqs. (21a) and (21b) into eq. (20), and expanding $\nabla^s \cdot (\sigma \mathbf{I^s})$ through the following identity (Starnoni, 2017)

$$\nabla^s \cdot (\sigma \mathbf{I}^s) = \nabla^s \sigma + \sigma k \mathbf{n}, \tag{22}$$

where k is the mean curvature of the surface given by (Aris, 1962)

$$k = -(\nabla^s \cdot \mathbf{n}), \tag{23}$$

the momentum balance for the surface $\mathcal{S} = nw$ dividing the wetting and non-wetting phases becomes

$$\begin{aligned} &\rho_{nw} \frac{D_s \mathbf{u}_{nw}}{Dt} - \nabla^s \sigma - \sigma k \mathbf{n}_{nw} - \nabla^s \cdot \boldsymbol{\tau}_{nw} - \rho_s \mathbf{g} + (p_n - p_w)\mathbf{n}_{nw} - (\boldsymbol{\tau}_n - \boldsymbol{\tau}_w)\mathbf{n}_{nw} \\ &+ [\rho_n(\mathbf{u}_n - \mathbf{u}_{nw})(\mathbf{u}_n - \mathbf{u}_{nw}) - \rho_w(\mathbf{u}_w - \mathbf{u}_{nw})(\mathbf{u}_w - \mathbf{u}_{nw})]\mathbf{n}_{nw} = 0. \end{aligned} \tag{24}$$

Taking the dot product between eq. (24) and $\mathbf{I}_s$ and $\mathbf{n}_{nw}$ respectively, the tangential and

normal components of the momentum balance finally read

$$\begin{aligned}\nabla^s\sigma =&\mathbf{I}^s\rho_{nw}\frac{D_s\mathbf{u}_{nw}}{Dt} - \mathbf{I}^s(\nabla^s\cdot\tau_{nw}) - \mathbf{I}^s\rho_{nw}\mathbf{g} - \mathbf{I}^s(\tau_n-\tau_w)\mathbf{n}_{nw}\\ &+\mathbf{I}^s[\rho_n(\mathbf{u}_n-\mathbf{u}_{nw})(\mathbf{u}_n-\mathbf{u}_{nw}) - \rho_w(\mathbf{u}_w-\mathbf{u}_{nw})(\mathbf{u}_w-\mathbf{u}_{nw})]\mathbf{n}_{nw},\end{aligned} \tag{25a}$$

$$\begin{aligned}p_n-p_w =&-\rho_{nw}\frac{D_s\mathbf{u}_{nw}}{Dt}\cdot\mathbf{n}_{nw}+\sigma k+(\nabla^s\cdot\tau_{nw})\cdot\mathbf{n}_{nw}+\rho_{nw}\mathbf{g}\cdot\mathbf{n}_{nw}+\mathbf{n}_{nw}\cdot(\tau_n-\tau_w)\mathbf{n}_{nw}\\ &-\mathbf{n}_{nw}\cdot[\rho_n(\mathbf{u}_n-\mathbf{u}_{nw})(\mathbf{u}_n-\mathbf{u}_{nw})-\rho_w(\mathbf{u}_w-\mathbf{u}_{nw})(\mathbf{u}_w-\mathbf{u}_{nw})]\mathbf{n}_{nw}.\end{aligned} \tag{25b}$$

It is important to note that no assumptions on the nature of the flow nor on the properties of the fluids have been made so far, thus equations (25a) and (25b) have to be considered always valid. In particular, eq. (25b) written as

$$p_n - p_w = \sigma k + \boldsymbol{\lambda}_s\cdot\mathbf{n}_{nw}, \tag{26}$$

where the vector $\boldsymbol{\lambda}_s$ accounts for all the momentum balance terms other than the adjacent fluids pressures, can be interpreted as an extension of the Young-Laplace equation to the dynamic case. For the most general case, $\boldsymbol{\lambda}_s$ is given by the following combination of terms

$$\boldsymbol{\lambda}_s = \boldsymbol{\lambda}_\rho + \boldsymbol{\lambda}_{\tau_s} + \boldsymbol{\lambda}_g + \boldsymbol{\lambda}_\tau + \boldsymbol{\lambda}_{\mathbf{u}_s}, \tag{27}$$

where

$$\boldsymbol{\lambda}_\rho = -\rho_s\frac{D_s\mathbf{u}_s}{Dt}, \tag{28a}$$

$$\boldsymbol{\lambda}_{\tau_s} = (\nabla^s\cdot\tau_s), \tag{28b}$$

$$\boldsymbol{\lambda}_g = \rho_s\mathbf{g}, \tag{28c}$$

$$\boldsymbol{\lambda}_\tau = (\tau_n-\tau_w)\mathbf{n}_{nw}, \tag{28d}$$

$$\boldsymbol{\lambda}_{\mathbf{u}_s} = -[\rho_n(\mathbf{u}_n-\mathbf{u}_s)(\mathbf{u}_n-\mathbf{u}_s)-\rho_w(\mathbf{u}_w-\mathbf{u}_s)(\mathbf{u}_w-\mathbf{u}_s)]\mathbf{n}_{nw}. \tag{28e}$$

Considering the surface massless ($\boldsymbol{\lambda}_\rho = \boldsymbol{\lambda}_g = 0$), neglecting the viscous part of the interface stress tensor ($\boldsymbol{\lambda}_{\tau_s} = 0$) and assuming no fluid exchange between the interface and the surroundings ($\boldsymbol{\lambda}_{\mathbf{u}_s} = 0$), the normal component of the momentum balance simplifies to

$$p_n - p_w = \sigma k + \boldsymbol{\lambda}_\tau\cdot\mathbf{n}_{nw}. \tag{29}$$

This latter simplified form of the microscopic momentum balance for a surface was also derived by Hassanizadeh and Gray (1993). The Young-Laplace equation (2) is only recovered with further neglection of the net viscous stress between the adjacent bulk phases ($\lambda_\tau = 0$) while, under all these assumptions, eq. (25a) eventually leads to $\nabla^s \sigma = 0$.

4 Classical macroscopic capillary pressure theories

4.1 Standard approach

Although almost universally used in macro-scale applications of two-phase flow in porous media, eq. (3) has two major inconsistencies. The first one is related to the scale of the averaging measures. In fact, it does not seem possible to obtain eq. (3) from a rigorous averaging of the relevant microscopic conservation equations. Moreover, eq. (24) is only valid at the interface and therefore its averaging would yield surface averages rather than intrinsic averages over the REV such as the ones appearing in eq. (3). An attempt to derive a macroscopic definition of capillary pressure through surface averaging was made by Whitaker (1986b). He took the surface average of the normal component of the microscopic momentum equation for a surface, eq. (29), and employed volume spatial decomposition to obtain

$$\langle p_n \rangle^n - \langle p_w \rangle^w = \sigma \langle k \rangle^{nw} + \mathcal{O}\left(\frac{\mu_i \langle \mathbf{u}_i \rangle^i}{d_i} \right), \tag{30}$$

where the subscript i refers to the largest contribution from the two fluid phases and d_i is the characteristic length scale of phase i. This formulation for the macroscopic capillary pressure clearly highlights this averaging incongruity: eq. (30) has intrinsic volume averages on the left hand side, but surface averages on the right hand side. Another weak point of this relationship is the fact that the spatial distribution of different orientated interfaces which may be present in a real porous material are not taken into account, instead they simply give the magnitude of the resultant force per total interfacial area. For these reasons, as already pointed out by Scheidegger (1963), formulations of such a kind seems to be suitable only for a single capillary or at best for a porous geometry formed by an assemblage of parallel tubes.

The second inconsistency of eq. (3) comes from dynamic considerations. In sec.

3 it has been shown that even at the microscopic level dynamic effects neglected by the Young-Laplace equation can play a role under certain circumstances, and that the Young-Laplace equation must be seen merely as a condition of thermodynamic equilibrium. At the macroscopic level this is exacerbated. The movement of one or more interfaces within a porous medium involves changes in phase saturations, interfacial areas and interfacial curvatures, as well as local mechanisms such as contact-angle hysteresis, snap-off and Haines jumps, which may provoke abrupt jumps in the interface configuration. Reducing all these features to the difference in the intrinsic average bulk pressures only appears to be a rather implausible simplification.

4.2 Thermodynamic approach

Alternative definitions of the macroscopic capillary pressure can be obtained using thermodynamic principles. Here, we present only some of these definitions. A much more extensive overview of these theories can be found in Hassanizadeh and Gray (1993). Morrow (1970) applied the first principle of thermodynamics to an idealized system for reversible immiscible displacement and obtained

$$\mathcal{P}_c = -\sum_{\alpha\beta} \sigma_{\alpha\beta} \frac{da_{\alpha\beta}}{d\forall_w} = -\sum_{\alpha\beta} \frac{\sigma_{\alpha\beta}}{\phi} \frac{d\hat{a}_{\alpha\beta}}{ds_w}, \quad \alpha\beta = nw, nk, wk \tag{31}$$

where ϕ is the porosity. This expression for the macroscopic capillary pressure has two main problems: the first one was recognized by Morrow himself, who pointed out that this relationship cannot be applied to a real porous medium as changes in volume and interfacial area do not take place reversibly. The second one is that eq. (31) does not consider any change in free energy of the bulk phases.

A step forward was made by Allen (1986) who applied the second law of thermodynamics to the system formed by the bulk phases to obtain

$$\mathcal{P}_c = -s_w \rho_w \frac{\partial A_w}{\partial s_w} + s_n \rho_n \frac{\partial A_n}{\partial s_n}, \tag{32}$$

where A_α, $\alpha = n, w$ is the Helmhotz free energy per unit mass of phase α. However, this definition is incomplete since it does not include any contribution from the interfaces.

A broader definition was given by Hassanizadeh and Gray (1990) and Gray and Has-

sanizadeh (1991) in the framework of a thermodynamic theory of two-phase flow in porous media. They started from the macroscopic mass, momentum, energy and entropy conservation equations for a bulk phase and for an interface. They then formulated constitutive hypotheses on the dependence of the Helmhotz free energies of the bulk phases and the interfaces on certain state variables such as density, phase saturation, temperature, interfacial area and porosity. Next, combining the second law of thermodynamics with the mass, energy and entropy conservation equations, they recovered a combination of terms contributing to the entropy inequality for the whole system, which for isothermal conditions and in absence of any other thermodynamic forces satisfies

$$\dot{s}_w \left[\mathcal{P}_w - \mathcal{P}_n - s_w \rho_w \frac{\partial A_w}{\partial s_w} + s_n \rho_n \frac{\partial A_n}{\partial s_n} - \sum_{\alpha\beta} \frac{\hat{a}_{\alpha\beta} \rho_{\alpha\beta}}{\phi} \frac{\partial A_{\alpha\beta}}{\partial s_w} \right] \geq 0, \quad \alpha\beta = nw, nk, wk \tag{33}$$

where $\dot{s}_w$ is the material time derivative of the saturation of the wetting phase, $A_{\alpha\beta}$ is the Helmhotz free energy per unit mass of interface $\alpha\beta$ and the macroscopic pressure $\mathcal{P}_\alpha$ is given by the following thermodynamic definition

$$\mathcal{P}_\alpha = (\rho_\alpha)^2 \frac{\partial A_\alpha}{\partial \rho_\alpha}. \qquad \alpha = n, w \tag{34}$$

This thermodynamically defined pressure, involving the change in energy with respect to volume, is often assumed to be equal to the physically measurable pressure, related to the trace of the stress tensor. This assumption holds under certain conditions such as a small rate of deformation tensor for a fluid. A physical interpretation of these different pressure measures can be found in Bennethum and Weinstein (2004).

Rearranging eq. (33) as

$$-\dot{s}_w[(\mathcal{P}_n - \mathcal{P}_w) - \mathcal{P}_c] \geq 0, \tag{35}$$

the following definition for the macroscopic capillary pressure $\mathcal{P}_c$ was then proposed (Hassanizadeh and Gray, 1990):

$$\mathcal{P}_c = -s_w \rho_w \frac{\partial A_w}{\partial s_w} + s_n \rho_n \frac{\partial A_n}{\partial s_n} - \sum_{\alpha\beta} \frac{\hat{a}_{\alpha\beta} \rho_{\alpha\beta}}{\phi} \frac{\partial A_{\alpha\beta}}{\partial s_w}. \tag{36}$$

According to this definition, the macroscopic capillary pressure is thus related to the

changes in free energy of both the bulk phases and the interfaces present within the system. If one takes the macroscopic interfacial tension $\sigma_{\alpha\beta}$ as (Hassanizadeh and Gray, 1990)

$$\sigma_{\alpha\beta} = -\hat{a}_{\alpha\beta}\rho_{\alpha\beta}\frac{\partial A_{\alpha\beta}}{\partial \hat{a}_{\alpha\beta}}, \tag{37}$$

and having postulated the dependence of $A_{\alpha\beta}$ on $\hat{a}_{\alpha\beta}$, application of the cyclic chain rule to the last term in eq. (36) yields

$$\sum_{\alpha\beta}\frac{\hat{a}_{\alpha\beta}\rho_{\alpha\beta}}{\phi}\frac{\partial A_{\alpha\beta}}{\partial s_w} = -\sum_{\alpha\beta}\frac{\hat{a}_{\alpha\beta}\rho_{\alpha\beta}}{\phi}\frac{\partial A_{\alpha\beta}}{\partial \hat{a}_{\alpha\beta}}\frac{\partial \hat{a}_{\alpha\beta}}{\partial s_w} = \sum_{\alpha\beta}\frac{\sigma_{\alpha\beta}}{\phi}\frac{\partial \hat{a}_{\alpha\beta}}{\partial s_w}, \tag{38}$$

so that eq. (36) becomes

$$\mathcal{P}_c = -s_w\rho_w\frac{\partial A_w}{\partial s_w} + s_n\rho_n\frac{\partial A_n}{\partial s_n} - \sum_{\alpha\beta}\frac{\sigma_{\alpha\beta}}{\phi}\frac{\partial \hat{a}_{\alpha\beta}}{\partial s_w}, \tag{39}$$

which resembles the definition obtained by Morrow, eq. (31), except that Morrow did not consider the changes in free energy of the bulk phases and thus only the last term of eq. (39) arises in his formulation. On the other hand, if this "Morrow's term" is neglected in eq. (39), one recovers Allen's definition, eq. (32). In fact, eq. (39) can be interpreted as a combination of these two works, or, the other way, eqs. (31) and (32) are special cases of eq. (39). However, these definitions still present one major inconvenience, that is they result from constitutive hypotheses which are axiomatically introduced by the Authors at the macro-scale. This would not be a problem in itself, since porous media have been traditionally studied and characterized at the macro-scale. However, recent numerical studies have shown that the macroscopic behaviour of a porous medium and its components is strongly dictated by the processes occurring at the pore-scale (e.g. Pruess et al. (2004)). Hence, we believe that definition of macro-scale quantities should follow naturally from their pore-scale counterparts, without introducing any assumptions on the macroscopic behaviour other than length-scale considerations.

5 Proposed definition of macroscopic capillary pressure

The microscopic momentum conservation equation for the surface nw, eq. (24), is rewritten as

$$\frac{\partial}{\partial t}(\rho_{nw}\mathbf{u}_{nw}) + \nabla^s\cdot(\rho_{nw}\mathbf{u}_{nw}\mathbf{u}_{nw}) - \nabla^s\sigma - \sigma k\mathbf{n}_{nw} - \nabla^s\cdot\boldsymbol{\tau}_{nw} - \rho_{nw}\mathbf{g} + (p_n - p_w)\mathbf{n}_{nw} - (\boldsymbol{\tau}_n - \boldsymbol{\tau}_w)\mathbf{n}_{nw} + [\rho_n\mathbf{u}_n(\mathbf{u}_n - \mathbf{u}_{nw}) - \rho_w\mathbf{u}_w(\mathbf{u}_w - \mathbf{u}_{nw})]\mathbf{n}_{nw} = 0. \tag{40}$$

The superficial surface average of eq. (40) is taken as

$$\begin{aligned}&\frac{1}{\forall}\int_{\mathcal{S}_{nw}}\frac{\partial}{\partial t}(\rho_{nw}\mathbf{u}_{nw})dA + \frac{1}{\forall}\int_{\mathcal{S}_{nw}}\nabla^s\cdot(\rho_{nw}\mathbf{u}_{nw}\mathbf{u}_{nw})dA - \frac{1}{\forall}\int_{\mathcal{S}_{nw}}\nabla^s\sigma dA\\ &- \frac{1}{\forall}\int_{\mathcal{S}_{nw}}\sigma k\mathbf{n}_{nw}dA - \frac{1}{\forall}\int_{\mathcal{S}_{nw}}\nabla^s\cdot\boldsymbol{\tau}_{nw}dA - \frac{1}{\forall}\int_{\mathcal{S}_{nw}}\rho_{nw}\mathbf{g}dA + \frac{1}{\forall}\int_{\mathcal{S}_{nw}}(p_n - p_w)\mathbf{n}_{nw}dA\\ &- \frac{1}{\forall}\int_{\mathcal{S}_{nw}}(\boldsymbol{\tau}_n - \boldsymbol{\tau}_w)\mathbf{n}_{nw}dA + \frac{1}{\forall}\int_{\mathcal{S}_{nw}}[\rho_n\mathbf{u}_n(\mathbf{u}_n - \mathbf{u}_{nw}) - \rho_w\mathbf{u}_w(\mathbf{u}_w - \mathbf{u}_{nw})]\mathbf{n}_{nw}dA = 0.\end{aligned} \tag{41}$$

Applying averaging theorems (16a) through (16c) to eq. (41) and using id. (15) yield

$$\begin{aligned}&\frac{\partial}{\partial t}(\hat{a}_{nw}\rho_{nw}\langle\mathbf{u}_{nw}\rangle^{nw}) + \nabla\cdot(\hat{a}_{nw}\rho_{nw}\langle\mathbf{u}_{nw}\rangle^{nw}\langle\mathbf{u}_{nw}\rangle^{nw}) + \nabla\cdot(\hat{a}_{nw}\rho_{nw}\langle\tilde{\mathbf{u}}_{nw}\tilde{\mathbf{u}}_{nw}\rangle^{nw})\\ &- \nabla(\hat{a}_{nw}\langle\sigma\rangle^{nw}) + \nabla\cdot(\hat{a}_{nw}\langle\mathbf{n}_{nw}\mathbf{n}_{nw}\sigma\rangle^{nw}) - \nabla\cdot(\hat{a}_{nw}\langle\boldsymbol{\tau}^s_{nw}\rangle^{nw}) - \hat{a}_{nw}\rho_{nw}\mathbf{g}\\ &+ \hat{a}_{nw}\langle(p_n - p_w)\mathbf{n}_{nw}\rangle^{nw} - \hat{a}_{nw}\langle(\boldsymbol{\tau}_n - \boldsymbol{\tau}_w)\mathbf{n}_{nw}\rangle^{nw} + \hat{a}_{nw}\langle[\rho_n\mathbf{u}_n(\mathbf{u}_n - \mathbf{u}_{nw})\\ &- \rho_w\mathbf{u}_w(\mathbf{u}_w - \mathbf{u}_{nw})]\mathbf{n}_{nw}\rangle^{nw} + \frac{1}{\forall}\int_{\mathcal{C}}[\rho_{nw}\mathbf{u}_{nw}(\mathbf{u}_{nw} - \mathbf{w})\cdot\mathbf{m} - \sigma\mathbf{m} + \boldsymbol{\tau}_{nw}\mathbf{m}]\,dC = 0.\end{aligned} \tag{42}$$

This is the form of the macroscopic momentum balance for the fluid-fluid interfaces originally derived by Gray and Hassanizadeh (1989) in their seminal work on the averaging theorems for transport of interface properties. Applying surface spatial decomposition (13) to the pressures in eq. (42), the macroscopic momentum balance is rearranged as follows

$$\hat{a}_{nw}\mathcal{P}_c\langle\mathbf{n}_{nw}\rangle^{nw} = \nabla(\hat{a}_{nw}\langle\sigma\rangle^{nw}) - \nabla\cdot(\hat{a}_{nw}\langle\mathbf{n}_{nw}\mathbf{n}_{nw}\sigma\rangle^{nw}) + \Lambda_s, \tag{43}$$

where $\mathcal{P}_c$ is the macroscopic capillary pressure defined as

$$\mathcal{P}_c = \langle p_n \rangle^{nw} - \langle p_w \rangle^{nw}, \tag{44}$$

and Λ_s is defined in analogy with the microscopic quantity λ_s used for the microscopic capillary pressure in Sec. 3, as

$$\Lambda_s = \Lambda_\rho + \Lambda_{\tau_s} + \Lambda_g + \Lambda_{\tilde{p}} + \Lambda_\tau + \Lambda_{\mathbf{u}_s} + \Lambda_c, \tag{45}$$

with

$$\begin{aligned}
\Lambda_\rho =& -\frac{\partial}{\partial t}(\hat{a}_{nw}\rho_{nw}\langle \mathbf{u}_{nw}\rangle^{nw}) - \nabla\cdot(\hat{a}_{nw}\rho_{nw}\langle \mathbf{u}_{nw}\rangle^{nw}\langle \mathbf{u}_{nw}\rangle^{nw}) \\
& - \nabla\cdot(\hat{a}_{nw}\rho_{nw}\langle \tilde{\mathbf{u}}_{nw}\tilde{\mathbf{u}}_{nw}\rangle^{nw}),
\end{aligned} \tag{46a}$$

$$\Lambda_{\tau_s} = \nabla\cdot(\hat{a}_{nw}\langle \boldsymbol{\tau}^s_{nw}\rangle^{nw}), \tag{46b}$$

$$\Lambda_g = \hat{a}_{nw}\rho_{nw}\mathbf{g}, \tag{46c}$$

$$\Lambda_{\tilde{p}} = -\hat{a}_{nw}\langle(\tilde{p}_n - \tilde{p}_w)\mathbf{n}_{nw}\rangle^{nw}, \tag{46d}$$

$$\Lambda_\tau = \hat{a}_{nw}\langle(\boldsymbol{\tau}_n - \boldsymbol{\tau}_w)\mathbf{n}_{nw}\rangle^{nw}, \tag{46e}$$

$$\Lambda_{\mathbf{u}_s} = -\hat{a}_{nw}\langle[\rho_n\mathbf{u}_n(\mathbf{u}_n - \mathbf{u}_{nw}) - \rho_w\mathbf{u}_w(\mathbf{u}_w - \mathbf{u}_{nw})]\mathbf{n}_{nw}\rangle^{nw}, \tag{46f}$$

$$\Lambda_c = -\frac{1}{\forall}\int_{\mathcal{C}}[\rho_{nw}\mathbf{u}_{nw}(\mathbf{u}_{nw} - \mathbf{w})\cdot\mathbf{m} - \sigma\mathbf{m} + \boldsymbol{\tau}_{nw}\mathbf{m}]\,dC. \tag{46g}$$

This definition of the macroscopic capillary pressure as the difference between intrinsic surface averages of the phase pressures is not found elsewhere in the literature. A similar one is given in the book by Gray and Miller (2014) in eq. 11.29. However, this term called P^{wn} is not assigned the meaning of macroscopic capillary pressure. Instead, these Authors define capillary pressure at the micro-scale as the product between interfacial tension and interfacial curvature, then bring this definition to the macro-scale. As far as the formulation of the macroscopic momentum balance equation for all the nw interfaces contained within the REV is concerned, it has three major merits. Firstly, it contains macroscopic variables obtained by rigorous application of integration theorems to their microscopic counterparts. Moreover, use of the Dirac function in eq. (12) allows for conveniently converting surface integrals into volume integrals and therefore carrying out averaging over the whole averaging volume. The latter aspect is particularly relevant

if one wants to remove the scale inconsistency of traditional definitions of macroscopic capillary pressure. Secondly, no assumptions on the flow regime nor on the properties of the different phases have been made. Hence, eq. (43) has to be considered valid for all possible flow conditions, static or dynamic, laminar or turbulent, as well as regardless of the compressibility of the fluids. In this regard, eq. (43) can be interpreted as a macroscopic generalized Young-Laplace equation. Finally, the presence of the intrinsic surface average of interface normal vectors, $\langle \mathbf{n}_{nw} \rangle^{nw}$, in the macroscopic capillary pressure term in the left hand side of eq. (43) permits to consider the actual spatial configuration of the various interfaces which may be present in real complex porous microstructures.

If now one introduces the following set of common simplifications for two-phase flow in porous media:

- No material interchange between the interface and the surrounding, i.e. $\Lambda_{\mathbf{u}_s} = 0$,
- Inertial forces are negligible, i.e. $\Lambda_\rho = 0$,
- Gravity effects on the interface are neglected $\Lambda_g = 0$,
- The viscous part of the interface stress tensor is neglected, i.e. $\Lambda_{\tau_s} = 0$,
- Constant interfacial tension,

the macroscopic momentum balance becomes

$$\begin{aligned} \hat{a}_{nw} \mathcal{P}_c \langle \mathbf{n}_{nw} \rangle^{nw} =& \sigma \left[\nabla \hat{a}_{nw} - \nabla \cdot (\hat{a}_{nw} \langle \mathbf{n}_{nw} \mathbf{n}_{nw} \rangle^{nw}) + \frac{1}{\forall} \int_{\mathcal{C}} \mathbf{m} dC \right] \\ &+ \Lambda_{\tilde{p}} + \Lambda_\tau. \end{aligned} \tag{47}$$

The term in square brackets multiplying σ can be simplified by noting that applying theorem (16b) to the constant scalar quantity $\psi_s = 1$ defined on a surface $\mathcal{S}$, yields

$$\int_{\mathcal{C}} \mathbf{m} dC = -\nabla a_s + \nabla \cdot (a_s \langle \mathbf{n}_s \mathbf{n}_s \rangle^s) + a_s \langle k \mathbf{n}_s \rangle^s. \tag{48}$$

By incorporating the latter result into eq. (47), the macroscopic momentum balance takes the form

$$\hat{a}_{nw} \mathcal{P}_c \langle \mathbf{n}_{nw} \rangle^{nw} = \hat{a}_{nw} \sigma \langle k \mathbf{n}_{nw} \rangle^{nw} + \Lambda_{\tilde{p}} + \Lambda_\tau. \tag{49}$$

The same result would have been obtained if the term $\nabla^s\sigma$ had been neglected in the first instance in eq. (40). The last two terms in eq. (49) can be estimated as (Whitaker, 1986a,b, 1998)

$$\Lambda_{\tilde{p}} + \Lambda_\tau = -\hat{a}_{nw}\langle(\tilde{p}_n - \tilde{p}_w)\mathbf{n}_{nw}\rangle^{nw} + \hat{a}_{nw}\langle(\boldsymbol{\tau}_n - \boldsymbol{\tau}_w)\mathbf{n}_{nw}\rangle^{nw} = \mathcal{O}\left(\frac{\mu_i\langle\mathbf{u}_i\rangle^i}{d_i^2}\right), \tag{50}$$

where the same length-scale considerations which led to eq. (30) have been used. By incorporating this result into eq. (49), the macroscopic momentum balance takes its final form

$$\hat{a}_{nw}\mathcal{P}_c\langle\mathbf{n}_{nw}\rangle^{nw} = \hat{a}_{nw}\sigma\langle k\mathbf{n}_{nw}\rangle^{nw} + \mathcal{O}\left(\frac{\mu_i\langle\mathbf{u}_i\rangle^i}{d_i^2}\right). \tag{51}$$

This form of the macroscopic capillary pressure resembles the one obtained by Whitaker (1986b), eq. (30), with two major distinctions. The first one lays in the fact that eq. (30) is in scalar form while eq. (51) is in vector form. This difference comes from the more rigorous approach chosen for averaging the relevant microscopic conservation equations. Whitaker took the average of only the normal component of the surface microscopic momentum balance, eq. (26), while here averaging of all the three components of the microscopic momentum balance for the surface, eq. (24), is carried out over the whole averaging volume through use of the Dirac function. The second distinction is the use of the intrinsic surface average to define the macroscopic capillary pressure in eq. (44). As already pointed out, Whitaker instead employed intrinsic volume averages. This difference in averaging measures arises from the different choice in applying spatial decomposition to the pressure terms. Although it is acknowledged that spatial decomposition is a fictitious treatment of the microscopic quantities made by the authors, nevertheless it does seem more rigorous to be consistent with the averaging domain over which averaging has been carried out. Since averaging in eq. (42) is taken over interfacial areas, intrinsic surface averages are used. The two approaches coincide only if the wetting and the non-wetting phase have constant pressure within the averaging volume.

6 A numerical example

6.1 Numerical method

The equations of flow are solved using classical CFD methods coupled with the Volume-of-Fluid (VOF) method for tracking the interfaces, following the approach of Raeini et al. (2012). In a VOF-Finite Volume framework, an indicator function η is defined for each cell as the ratio between the volume of fluid 1 contained within the cell, V^η, and the volume of the cell V as

$$\eta = \frac{V^\eta}{V}. \tag{52}$$

This means that the indicator function is bounded between 0 and 1 as follows

$$\eta = \begin{cases} 1, & \text{if the cell is filled with fluid 1,} \\ 0, & \text{if the cell is filled with fluid 2,} \\ 0 < \eta < 1, & \text{if there is an interface within the cell.} \end{cases} \tag{53}$$

Starting from a known initial distribution, the volume fraction is updated in time by solving the following advection equation

$$\frac{\partial \eta}{\partial t} + \nabla \cdot (\eta \mathbf{u}) = \eta \nabla \cdot \mathbf{u}, \tag{54}$$

where t is time and $\mathbf{u}$ is the velocity vector. We employed the Piecewise Linear Interface Calculation (PLIC) method by Youngs (1982) to solve eq. (54) numerically. In the PLIC method, the interface is mathematically described as a planar surface defined by equation

$$\mathbf{n} \cdot \mathbf{x} - \chi = 0, \tag{55}$$

where χ is a constant determined by matching the interface truncated volume $V(\mathbf{n}, \chi)$ to the actual fluid volume V^η contained in the cell, and $\mathbf{n}$ is the interface unit normal vector pointing outwards from fluid 1:

$$\mathbf{n} = -\frac{\nabla \eta}{|\nabla \eta|}. \tag{56}$$

The flow variables p and $\mathbf{u}$ are obtained by solving the Navier-Stokes equations with surface tension forces

$$\frac{\partial}{\partial t}(\rho \mathbf{u}) + \nabla \cdot (\rho \mathbf{u}\mathbf{u}) + \nabla p - \nabla \cdot \boldsymbol{\tau} - \rho \mathbf{g} - \mathbf{f}_s = 0, \tag{57}$$

where $\boldsymbol{\tau} = \mu \left[\nabla \mathbf{u} + (\nabla \mathbf{u})^T\right]$ is the viscous stress tensor, $\mathbf{g}$ is the gravitational acceleration, $\mathbf{f}_s$ is the surface tension force, and ρ and μ are the average density and viscosity, which in the VOF method are computed from the properties of the fluids 1 and 2 as

$$\begin{aligned} \rho &= \eta \rho_1 + (1 - \eta)\, \rho_2, \\ \mu &= \eta \mu_1 + (1 - \eta)\, \mu_2. \end{aligned} \tag{58}$$

Following the Continuous Surface Force (CSF) model by Brackbill et al. (1992), the surface tension force $\mathbf{f}_s$ is computed as a body force using the Dirac delta function δ_s concentrated at the interface as follows:

$$\mathbf{f}_s = \sigma k \mathbf{n} \delta_s, \tag{59}$$

where σ is the interfacial tension, k is the interface curvature defined as (Aris, 1962)

$$k = -\nabla \cdot \mathbf{n}, \tag{60}$$

and $\mathbf{n}$ is the unit normal to the interface computed using eq. (56). Equations (54) and (57) are solved using an in-house Finite Volume code. Full description of the numerical implementation can be found in Starnoni (2017).

6.2 Numerical setup

Drainage simulations are carried out on a porous region cropped from a three-dimensional (3D) digital image of a carbonate rock obtained from X-rays μ-CT. Details on the morphology and petrophysics of this rock can be found in Starnoni et al. (2017).

In our model, the image voxels, i.e. the voxel is the 3-D equivalent of a 2-D pixel, form the structured computational grid, that is the computational cell coincides with the image voxel. In these simulations, the computational domain constists of 100x40x40 grid cells of size 8.3 μm and porosity of 0.26. Values of interfacial tension σ and static contact

angle θ for supercritical CO_2-water systems are used (Espinoza and Santamarina, 2010). σ is taken equal to 0.04 N/m and $\theta = 30°$. For the sake of simplicity, the viscosity ratio is taken equal to 1. A numerical study on the effects of viscosity ratio on the two-phase flow dynamics in constricted pore-throat geometries can be found in Starnoni and Pokrajac (2018). Boundary conditions consist of prescribed pressure at the outlet and velocity equal to 5 mm/s at the inlet. As initial conditions, the non-wetting phase fills the initial 10% of the image next to the inlet boundary (initial saturation of the injected non-wetting phase $s_{nw}^0 = 0.11$). The time evolution of the VOF indicator function η can be visualized in Fig. 2 (final saturation at breakthrough $s_{nw}^f = 0.6$).

6.3 Comparison of different macroscopic capillary pressure measures

We make here a comparison between three macroscopic capillary pressure measures. The first one is the standard definition of $\mathcal{P}_c$, i.e. eq. (3), denoted as $\mathcal{P}_c^{standard}$, which is computed as

$$\mathcal{P}_c^{standard} = \langle p_n \rangle^n - \langle p_w \rangle^w = \frac{\sum p_i(1-\eta)V_i}{\sum(1-\eta)V_i} - \frac{\sum p_i \eta V_i}{\sum \eta V_i}, \tag{61}$$

where η is the indicator function defined in eq. (53), V is the volume of the cell, and the sum is over all the computational cells. The second one is the intrinsic surface average of the interface curvature, i.e. the right hand side of eq. (30). It is denoted as $\mathcal{P}_c^k$ and is computed as

$$\mathcal{P}_c^k = \sigma \langle k \rangle^{nw} = \sigma \frac{\sum k_i |\nabla \eta|_i V_i}{\sum |\nabla \eta|_i V_i}, \quad i \in \text{"Interface cells"}, \tag{62}$$

where the sum is now over the union of the cells containing an interface, i.e. $0 < \eta < 1$. Finally, the macroscopic capillary pressure computed from the intrinsice surface averages of the bulk pressures, eq. (44), denoted as $\mathcal{P}_c^{nw}$, is computed as

$$\mathcal{P}_c^{nw} = \langle p_n \rangle^{nw} - \langle p_w \rangle^{nw} = \frac{\sum p_i(1-\eta)V_i}{\sum(1-\eta)V_i} - \frac{\sum p_i \eta V_i}{\sum \eta V_i}, \quad i \in \text{"Interface cells"}, \tag{63}$$

where, as in eq. (62) the sum is only over the cells containing an interface. Hence, we have one expression where the sum is over all the computational cells, eq. (61), and two expressions where the sum is only over the interface cells, eqs. (62) and (63).

Fig. 3 shows the different computed macroscopic capillary pressure measures as a

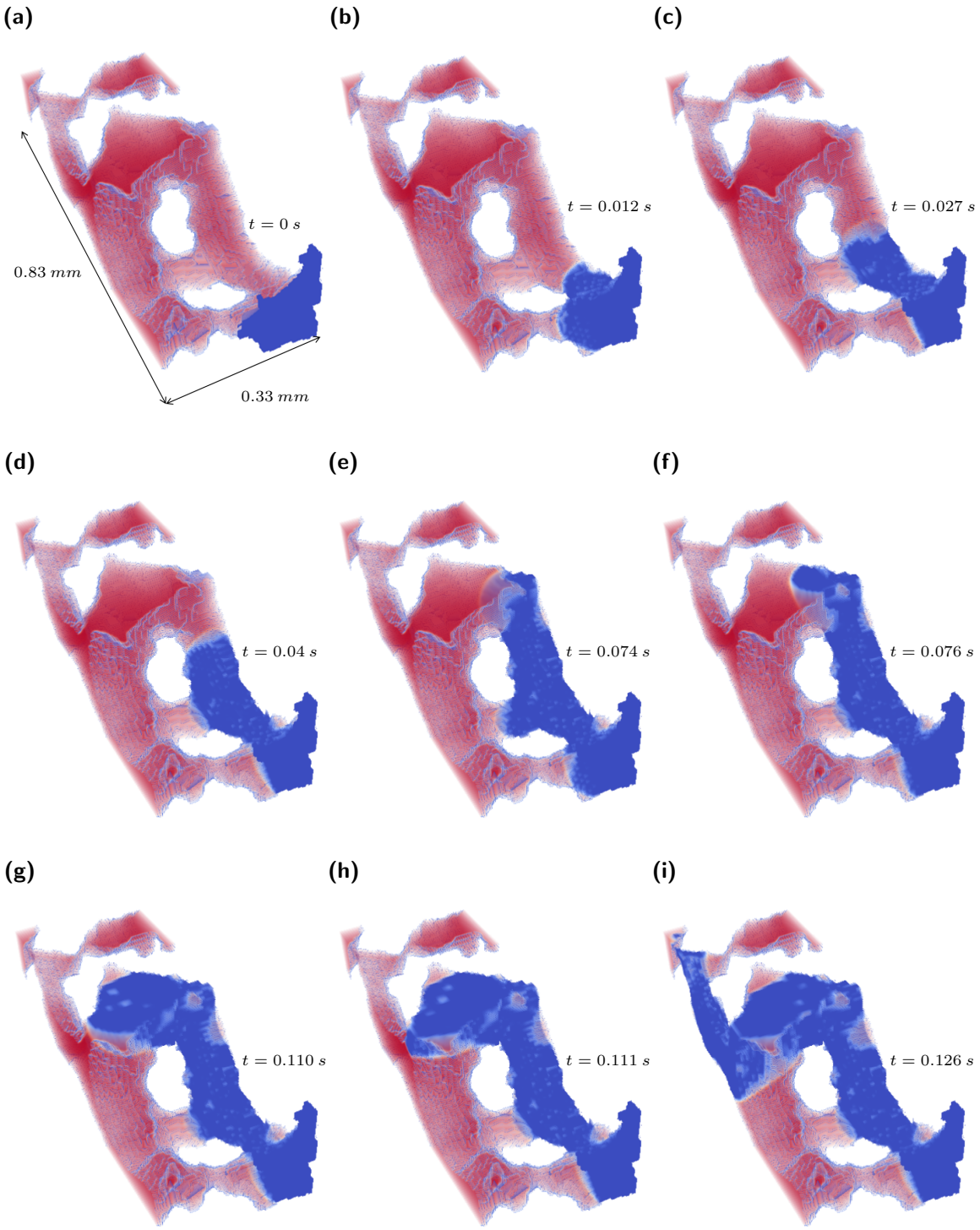

Figure 2. Time evolution of the VOF indicator function η. The non-wetting fluid is displayed in blue ($\eta = 0$) and the wetting fluid in red ($\eta = 1$).

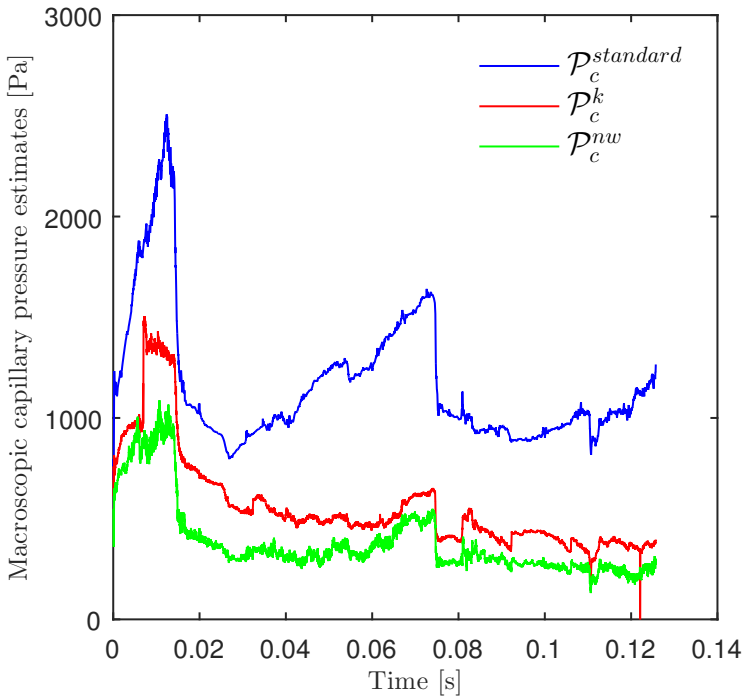

Figure 3. Comparison of different macroscopic capillary pressure measures

function of time. Overall the three curves behave similarly. However, a significant difference between the standard macroscopic capillary pressure, computed using eq. (61), and the other two measures, i.e. eqs. (62) and (63), is observed. This difference is due to the fact that $\mathcal{P}_c^{standard}$ is computed from a discretization of the intrinsic volume average operator, while the other two measures are computed from discretized surface averages. This means that in real porous media the pressure within each phase is not constant. On the other hand, better agreement is observed between $\mathcal{P}_c^{k}$ and $\mathcal{P}_c^{nw}$. This confirms the argument made in Sec. 5 that use of surface averages for the pressures is more appropriate than that of volume averages when averaging the relevant surface microscopic balance equations. It must be noted that our simulations are performed for a limited flow domain that does not satisfy requirements for REV. The reason is the prohibitevely high demand for computational time required by the simulations, and the complexity of the 3-D computational domain reflecting the real microstructure of a reservoir rock. This is clearly a limitation at the current state. However, we believe that in future, given the continuing advances in computer power, it will be possible to obtain capillary pressure-saturation relationships not from experiments but directly from numerical simulations, in a similar way to what is done for the absolute permeability in single-phase flow (Mostaghimi et al., 2013; Starnoni et al., 2017) and for the relative permeabilities-saturation curves in two-

phase flow (Raeini et al., 2014). In other words, it will be possible to obtain input data for field-scale simulations directly as outputs of pore-scale simulations. Our work shows that the averaging method to be used in this scenario should be surface averages rather than bulk averages.

7 Limitations of the proposed approach

Introduction of the new capillary pressure definition in terms of intrinsic surface averages implies a re-thinking of the classical approach employed in modelling two-phase flow at the reservoir-scale. On the other hand, at the reservoir scale, it was already known thay only capillary flow models can effectively describe the Sleipner field CO_2 plume evolution in the northern North Sea (Cavanagh and Nazarian, 2014), and early breakthrough at the Frio injection site is thought to be largely due to preferential capillary pressure pathways (Hovorka et al., 2006). Besides, code comparison studies (Pruess et al., 2004) have shown that the largest discrepancies between different simulators can be traced to uncertainties in macro-scale parameters such as absolute permeability, relative permeabilities, and capillary pressure. It is therefore clear that capillary pressure significantly impacts the flow and trapping of CO_2 from the pore to the laboratory to the field scale, and need to be accurately characterised and incorporated into subsurface modelling efforts.

While we believe that our methodology for calculating the macroscopic capillary pressure from results of pore-scale numerical simulations sets important perspectives for future investigations, though we identify three possible sources of limitations of our approach, namely 1) the relation between surface average pressure and the pressure appearing in Darcy's law, 2) the applicability of our method to non-standard real situations such as Haines jumps and thin film flow, and 3) the reliable delineation of an REV for the medium and its properties.

7.1 Relation between different pressure measures

Traditionally, numerical simulation models of reservoir-scale two-phase flow in porous media use mass conservation equation together with Darcy's law applied to each fluid. Darcy's law contains macroscopic pressure for each phase, i.e. (microscopic) pressure averaged over the volume occupied by each phase. The experimentally determined $\mathcal{P}_c(s_w)$

relationship then completes the set of equations. Macroscopic capillary pressure is traditionally taken as difference between bulk pressures (eq. (3)) simply because it is convenient to measure the pressures at the inlet and outlet of a core sample during traditional coreflooding experiments. If one then introduces the new macroscopic capillary pressure from the surface averages (eq. (44)), it is clear that either new equations are needed in the model, e.g. eq. (43), or the traditional $\mathcal{P}_c - s_w$ relationship has to be modified in order to account for the different pressure measures appearing in Darcy's law and in eq. (43). The former approach seems unfeasible in practice, since additional parameters would arise in these more advanced models, namely the interfacial surface area, the average curvature, and the average interface normal. Determination of these parameters can potentially be an enormous task. Regarding the latter approach, there already exist advanced models which, based on the work by Gray and Hassanizadeh (1991) and Hassanizadeh and Gray (1990), utilize a modified $\mathcal{P}_c - s_w$ relationship of the form:

$$\mathcal{P}_n - \mathcal{P}_w = \mathcal{P}_c(s_w) - \eta \frac{\partial s_w}{\partial t}, \tag{64}$$

where the left hand side contains the phase pressures appearing in Darcy's law, $\mathcal{P}_c$ is an intrinsic property of the porous medium-fluids system, and η is a dynamic capillarity coefficient. The addition of time derivatives or other driving forces into the macroscopic capillary pressure definition accounts for disequilibrium at the pore-scale during flow and is likely specific to a given problem. In some cases, this disequilibrium (the difference between macroscopic capillary pressure and phase pressure difference) is referred to as dynamic capillary pressure and is known to be a rate dependent effect (Weitz et al., 1987). It is clear that a formulation to account for disequilibrium is required since a relationship between the pressure difference between the non-wetting and wetting phase and the capillary pressure at an interface is usually determined for static conditions. We believe that our formulation may instead provide a useful means of evaluating this missing relationship. A straightforward incorporation of our approach in existing frameworks would therefore be to utilize the macroscopic capillary pressure from the surface averages $\mathcal{P}_c^{nw}$ as the intrinsic property of the porous medium-fluids system, and to provide its functional relationship with the fluid saturation using pore-scale simulation models or pore-scale experiments instead of traditional coreflooding experiments.

7.2 Local mechanisms

When discussing limitations of the standard definition of the macroscopic capillary pressure in Sec. 4.1, we mentioned examples of local mechanisms such as Haines jumps and snap-off, which would make the standard definition too simplistic. However, since our approach has not yet been verified through either numerical or experimental investigations, these limitations potentially still apply. An example of limitations of the proposed approach is a situation that occurs during Haines jumps, when a non-wetting phase invades a less geometrically constrained region of the pore space. Particularly, pore drainage events were observed to be cooperative, meaning that capillary pressure differences which extend over multiple pores directly affect fluid topology and menisci dynamics, suggesting that not only viscous forces but also capillarity acts in a nonlocal way (Armstrong and Berg, 2013). Besides, during the drainage of a porous rock a capillary dispersion zone is observed, over which the wetting phase saturation is reduced. The pressure gradient applied over the extent of the porous rock drives the macro-scale movement of the capillary dispersion zone forward. However, local transient pressure gradients within the capillary dispersion zone drive the progression of the dispersion zone. These transient pressure gradients occur during geometrical changes of interfaces, which create moments when the interfacial curvature of fluid-fluid interfaces is not constant (Armstrong et al., 2015).

Other examples where our approach may be limited are the condition of low saturation, when the effect of film flow prevails over capillary flow in dry porous media (Tuller and Or, 2001; Lebeau and Konrad, 2010), or flow in fractured porous media (Firoozabadi et al., 1990; Rangel-German et al., 2006).

7.3 Determination of the REV

The equations developed in this paper rely on the identification of an REV for the material over which integration of the pore-scale relevant equations is carried out. However, a reliable delineation of an REV for different porous media parameters is difficult or unattainable in practice, even for homogeneous media (Costanza-Robinson et al., 2011). An example of this difficulty follows from the example described in the previous section, where the zone of influence associated with a Haines jump was found to exist over a distance of multiple pores and thus is much larger than the correlation length for the

homogenous model pattern. This sets a lower limit for the size of an REV for dynamic conditions, i.e. when considering large local velocities that occur during Haines jumps, and demonstrates that this limit is larger than what would be measured by considering only the pore space geometry (e.g. porosity) (Armstrong et al., 2015).

8 Conclusions

We presented a novel definition of the macroscopic capillary pressure. This definition follows naturally from application of the method of volume averaging for transport of interface properties in multiphase systems. Starting from the microscopic momentum balance for a surface, we recalled the macroscopic momentum balance equation for all the fluid-fluid interfaces contained within an REV derived by Gray and Hassanizadeh (1989), and recast it in a form which can be interpreted as a generalized Young-Laplace equation at the macro-scale. This novel formulation resolves most of the shortcomings of the previous studies, such as the averaging-scale inconsistency, the lack of dynamic terms in the momentum balance, and the accounting for the different orientation of interfaces within the averaging volume. It also reveals another parameter, namely the intrisic surface average of the average normal vector, which may have significant effect on the dynamics of the fluid-fluid interfaces at macroscopic scale. However, its determination remains an open research question. Nevertheless, this approach could be very useful for interpreting results of pore-scale simulation models.

We also presented numerical results of drainage simulations on porous regions extracted from real reservoir rocks. Simulations results showed a significant difference between the standard definition of the macroscopic capillary pressure commonly employed in field-scale computational codes and other more rigorous forms employing intrinsic surface averages. Prediction of the flow variables from pore-scale simulations, as opposed to traditional coreflooding experiments, can therefore provide more rigorous $\mathcal{P}_c - s_w$ relationships. This sets new challenging perpspectives for reservoir engineering applications, and more generally for all engineering problems involving two-phase porous media flows. Constant advances in computer power will enable the implementation of multi-scale simulation models where the input data for field-scale simulations will be obtained by directly upscaling results of pore-scale simulations.

Acknowledgements

This work was jointly sponsored by EPSRC (EP/I010971/1) and NSFC China. The authors would like to acknowledge the support of the Maxwell computer cluster funded by the University of Aberdeen. Data used in this paper are properly cited and referred to in the reference list.

Bibliography

Allen, M. B. (1986). Mechanics of multiphase fluid flows in variably saturated porous media. *International Journal of Engineering Science*, 24(3):339–351.

Aris, R. (1962). *Vectors, tensors and the basic equations of fluid mechanics*. Prentice Hall, Englewood Cliffs.

Armstrong, R. T. and Berg, S. (2013). Interfacial velocities and capillary pressure gradients during haines jumps. *Physical Review E*, 88(4):043010.

Armstrong, R. T., Evseev, N., Koroteev, D., and Berg, S. (2015). Modeling the velocity field during haines jumps in porous media. *Advances in Water Resources*, 77:57–68.

Bear, J. (1972). *Dynamics of Fluids in Porous Media*. Elsevier.

Bear, J. and Verruijt, A. (1987). *Modeling Groundwater Flow and Pollution*, volume 2. D. Reidel.

Bennethum, L. S. and Weinstein, T. (2004). Three pressures in porous media. *Transport in Porous Media*, 54(1):1–34.

Brackbill, J., Kothe, D. B., and Zemach, C. (1992). A continuum method for modeling surface tension. *Journal of Computational Physics*, 100(2):335–354.

Brooks, R. H. and Corey, A. T. (1964). Hydraulic properties of porous media and their relation to drainage design. *Trans. ASAE*, 7(1):26–0028.

Cavanagh, A. and Nazarian, B. (2014). A new and extended sleipner benchmark model for co2 storage simulations in the utsira formation. *Energy Procedia*, 63:2831–2835.

Costanza-Robinson, M. S., Estabrook, B. D., and Fouhey, D. F. (2011). Representative elementary volume estimation for porosity, moisture saturation, and air-water interfacial areas in unsaturated porous media: Data quality implications. *Water Resources Research*, 47(7).

Deemer, A. R. and Slattery, J. C. (1978). Balance equations and structural models for

538 phase interfaces. *International Journal of Multiphase Flow*, 4(2):171–192.

539 Espinoza, D. N. and Santamarina, J. C. (2010). Water-co2-mineral systems: Interfa-
540 cial tension, contact angle, and diffusionimplications to co2 geological storage. *Water*
541 *Resources Research*, 46(7).

542 Firoozabadi, A., Hauge, J., et al. (1990). Capillary pressure in fractured porous me-
543 dia (includes associated papers 21892 and 22212). *Journal of Petroleum Technology*,
544 42(06):784–791.

545 Gray, W. G. and Hassanizadeh, S. (1989). Averaging theorems and averaged equations
546 for transport of interface properties in multiphase systems. *International Journal of*
547 *Multiphase Flow*, 15(1):81–95.

548 Gray, W. G. and Hassanizadeh, S. M. (1991). Unsaturated flow theory including interfacial
549 phenomena. *Water Resources Research*, 27(8):1855–1863.

550 Gray, W. G., Leijnse, A., Kolar, R. L., and Blain, C. A. (1993). *Mathematical tools for*
551 *changing scale in the analysis of physical systems*. CRC Press.

552 Gray, W. G. and Miller, C. T. (2014). *Introduction to the thermodynamically constrained*
553 *averaging theory for porous medium systems*. Springer.

554 Hassanizadeh, S. and Gray, W. G. (1993). Thermodynamic basis of capillary pressure in
555 porous media. *Water Resources Research*, 29(10):3389–3405.

556 Hassanizadeh, S. M. and Gray, W. G. (1990). Mechanics and thermodynamics of mul-
557 tiphase flow in porous media including interphase boundaries. *Advances in Water*
558 *Resources*, 13(4):169–186.

559 Hovorka, S. D., Benson, S. M., Doughty, C., Freifeld, B. M., Sakurai, S., Daley, T. M.,
560 Kharaka, Y. K., Holtz, M. H., Trautz, R. C., Nance, H. S., et al. (2006). Measuring
561 permanence of co2 storage in saline formations: the frio experiment. *Environmental*
562 *Geosciences*, 13(2):105–121.

563 Joekar-Niasar, V. and Hassanizadeh, S. (2011). Specific interfacial area: The missing
564 state variable in two-phase flow equations? *Water Resources Research*, 47(5).

565 Lebeau, M. and Konrad, J.-M. (2010). A new capillary and thin film flow model for
566 predicting the hydraulic conductivity of unsaturated porous media. *Water Resources*
567 *Research*, 46(12).

568 Morrow, N. R. (1970). Physics and thermodynamics of capillary action in porous media.
569 *Industrial & Engineering Chemistry*, 62(6):32–56.

570 Mostaghimi, P., Blunt, M. J., and Bijeljic, B. (2013). Computations of absolute perme-
571 ability on micro-ct images. *Mathematical Geosciences*, 45(1):103–125.
572 Pruess, K., García, J., Kovscek, T., Oldenburg, C., Rutqvist, J., Steefel, C., and Xu,
573 T. (2004). Code intercomparison builds confidence in numerical simulation models for
574 geologic disposal of co2. *Energy*, 29(9-10):1431–1444.
575 Raeini, A. Q., Blunt, M. J., and Bijeljic, B. (2012). Modelling two-phase flow in porous
576 media at the pore scale using the volume-of-fluid method. *Journal of Computational*
577 *Physics*, 231(17):5653–5668.
578 Raeini, A. Q., Blunt, M. J., and Bijeljic, B. (2014). Direct simulations of two-phase flow
579 on micro-ct images of porous media and upscaling of pore-scale forces. *Advances in*
580 *water resources*, 74:116–126.
581 Rangel-German, E., Akin, S., and Castanier, L. (2006). Multiphase-flow properties of
582 fractured porous media. *Journal of Petroleum Science and Engineering*, 51(3-4):197–
583 213.
584 Scheidegger, A. E. (1963). *Physics of Flow through Porous Media*. University of Toronto.
585 Starnoni, M. (2017). *Modelling single and two-phase flow on micro-CT images of rock*
586 *samples*. PhD thesis, University of Aberdeen.
587 Starnoni, M. and Pokrajac, D. (2018). Numerical study of the effects of contact angle and
588 viscosity ratio on the dynamics of snap-off through porous media. *Advances in Water*
589 *Resources*, 111:70–85.
590 Starnoni, M., Pokrajac, D., and Neilson, J. E. (2017). Computation of fluid flow and
591 pore-space properties estimation on micro-ct images of rock samples. *Computers &*
592 *Geosciences*, 106:118–129.
593 Tuller, M. and Or, D. (2001). Hydraulic conductivity of variably saturated porous media:
594 Film and corner flow in angular pore space. *Water Resources Research*, 37(5):1257–
595 1276.
596 Van Der Lee, J., De Windt, L., Lagneau, V., and Goblet, P. (2003). Module-oriented
597 modeling of reactive transport with hytec. *Computers & Geosciences*, 29(3):265–275.
598 Van Genuchten, M. T. (1980). A closed-form equation for predicting the hydraulic con-
599 ductivity of unsaturated soils. *Soil Science Society of America journal*, 44(5):892–898.
600 Weitz, D., Stokes, J., Ball, R., and Kushnick, A. (1987). Dynamic capillary pressure
601 in porous media: Origin of the viscous-fingering length scale. *Physical review letters*,

59(26):2967.

Whitaker, S. (1969). Advances in theory of fluid motion in porous media. *Industrial & Engineering Chemistry*, 61(12):14–28.

Whitaker, S. (1977). A theory of drying. *Advances in Heat Transfer*, 13:119–203.

Whitaker, S. (1986a). Flow in porous media i: A theoretical derivation of darcy's law. *Transport in Porous Media*, 1(1):3–25.

Whitaker, S. (1986b). Flow in porous media ii: The governing equations for immiscible, two-phase flow. *Transport in Porous Media*, 1(2):105–125.

Whitaker, S. (1998). *The Method of Volume Averaging*, volume 13. Springer Science & Business Media.

Xu, T., Spycher, N., Sonnenthal, E., Zhang, G., Zheng, L., and Pruess, K. (2011). Toughreact version 2.0: A simulator for subsurface reactive transport under non-isothermal multiphase flow conditions. *Computers & Geosciences*, 37(6):763–774.

Yeh, G. and Tripathi, V. S. (1990). *HYDROGEOCHEM: A coupled model of HYDROlogical transport and GEOCHEMical equilibria in reactive multicomponent systems*. Oak Ridge National Lab.

Youngs, D. L. (1982). Time-dependent multi-material flow with large fluid distortion. *Numerical Methods for Fluid Dynamics*, 24(2):273–285.